THE ASTROPHYSICAL JOURNAL 247:362–373, 1981 July 1

INTERPRETATION OF COSMIC RAY COMPOSITION: THE PATH LENGTH DISTRIBUTION

R. J. PROTHEROE,[1] J. F. ORMES, AND G. M. COMSTOCK[2]
Laboratory for High Energy Astrophysics, NASA Goddard Space Flight Center
Received 1980 July 21: accepted 1981 January 5

ABSTRACT

The chemical composition of cosmic ray nuclei with $3 \leq Z \leq 28$ between a few hundred MeV/nucleon and a few hundred GeV/nucleon is compared with a consistent set of propagation calculations. These include the effects of spallation (energy-dependent cross sections are used), escape, ionization loss in the interstellar medium, and deceleration in the solar cavity. The amount of matter traversed by cosmic rays is found to be ~ 7 g cm^{-2}, independent of energy between 100 MeV/nucleon and 2 GeV/nucleon. Above 2 GeV/nucleon, the escape length varies as $E^{-0.4 \pm 0.1}$. In addition, a procedure has been developed to measure the shape of the cosmic ray path length distribution.

Utilizing the ratio of Fe secondaries to Fe in the cosmic rays, presently available data are found to be consistent with an exponential distribution and to eliminate models in which the path length distribution is severely truncated. To tie down the shape of the distribution more precisely, new measurements of the cosmic ray composition presently becoming available from experiments on the *HEAO 3* satellite will have to be coupled with improved measurements of the energy dependence of partial and total cross sections.

Subject headings: cosmic rays: abundances — interstellar: matter

I. INTRODUCTION

The chemical composition of cosmic rays reflects information not only on the mean amount of matter traversed by the particles between their sources and the solar system, but also on the shape of the distribution of matter as sampled by the particles. As is well known, cosmic ray nuclei from sources (primaries) spall on traversing the matter in interstellar space, producing secondary nuclides. By studying the relative composition of heavier secondary nuclides which are rare or absent at the source, the shape (or moments) of the path length distribution can be studied. This shape reflects the location (either spatially or temporally) of sources relative to the observer (Owens 1976) and hence is important in understanding their origin.

In this paper we present calculations of the effects of the distribution of path lengths through which the cosmic rays propagate on the detailed chemical composition and compare these calculations with data from a variety of experiments ranging from 100 MeV/nucleon to 100 GeV/nucleon.

It has been generally believed that the composition was best explained by a path length distribution (PLD) with an absence of short path lengths. This was thought necessary to explain the large number of nuclei observed in the subiron region (Shapiro and Silberberg 1970; Shapiro, Silberberg, and Tsao 1973; Garcia-Munoz and Simpson 1970; Fichtel and Reames 1968). Since that time new measurements have been made of some of the cross sections involved. The mean matter traversed has been found to vary with energy, and more accurate charge composition measurements have been made.

There is a sound theoretical basis for a PLD in which short path lengths are absent. Lezniak and Webber (1979) have derived the PLD shapes expected in some of these models. In one such model some of the matter through which cosmic rays pass is located in the cosmic ray source. Cowsik and Wilson (1973, 1975) first invoked a "double or nested leaky box" model to explain the early observations of energy-dependent changes in the abundance ratios of primary cosmic rays. Simon (1977) introduced a convenient parametrization of the PLD resulting from these models in terms of the convolution of two exponential distributions. We utilize this formalism to investigate the shape of the PLD using the cosmic ray data.

In this paper, the available data will be compared with a self-consistent set of calculations. By comparing the data from different groups with the same model, any differences which might exist between calculations are eliminated in interpreting the data.

We will assume that acceleration of cosmic rays during their propagation in the interstellar medium is negligible and that the cosmic rays are effectively injected into the Galaxy with a power-law spectrum common to all species. This would apply if cosmic rays are accelerated in localized accelerators and then injected into the interstellar medium where the

[1] NAS/NRC Resident Research Associate.
[2] Cosmo-Science Associates, Stony Brook, NY.

probability of subsequent acceleration is small. This could be localized shocks (Blandford and Ostriker 1978; Jokipii and Higdon 1979), the acceleration of a thermal plasma to cosmic ray energies (Eichler 1980), or acceleration in supernova remnants (Scott and Chevalier 1975).

We begin with the simple leaky box model (Cowsik *et al.* 1967), a model of cosmic ray propagation in which the PLD is exponential. Using the observed relative abundance of the light secondary elements Be and B and the primary elements C and O, we can determine a mean escape length $\lambda_e(E)$ as a function of energy. The general features found by Ormes and Freier (1978) are present: a decreasing escape length at high energies (>2 GeV/nucleon), and a constant escape length at lower energies. Jones (1979) has shown that the general shape of $\lambda_e(E)$ can be explained by a galactic wind model (Jokipii 1976) in which escape of particles by diffusion dominates at high energies, while escape by convection dominates at low energy.

The effect of varying the shape of the PLD on the secondary nuclei in the range $21 \leq Z \leq 25$ just below the abundant primary iron nuclei is studied since the abundance of these elements is more sensitive to the shape of the PLD than the light secondary elements. Such studies are dependent upon a knowledge of the partial cross sections for producing each secondary isotope from every possible primary isotope. Insufficient measurements of the energy dependence of these important cross sections have been made, as noted by Raisbeck (1979), and care must therefore be taken when using these data. We use here the semi-empirical formulations of Silberberg and Tsao (1973*a*, *b*, 1977*a*, *b*, *c*; Tsao and Silberberg 1979), including all their corrections based upon the recent measurements with the Bevalac. The various versions of these formulations have been cross-checked with Silberberg and Tsao under a communitywide effort initiated by P. S. Freier. We shall discuss the limitations on the interpretations due to uncertainties in the cross sections.

II. METHOD OF CALCULATION

In the equilibrium steady-state homogeneous model, the intensity $J_i(E)$ of particles of type i at energy E is given by

$$Q_i(E) - \frac{J_i(E)}{\lambda_e{}^i(E)} - \frac{J_i(E)}{\lambda_{\rm dec}{}^i(E)} - \frac{J_i(E)}{\lambda_{\rm int}{}^i(E)} + \sum_{k \geq i} \left[\frac{J_k(E)}{\lambda_{\rm spall}{}^{ki}(E)} + \frac{J_k(E)}{\lambda_{\rm dec}{}^{ki}(E)} \right] - \frac{d}{dE}[w_i(E) J_i(E)] = 0 , \quad (1)$$

where Q_i is the source term; $\lambda_e{}^i$, $\lambda_{\rm dec}{}^i$, and $\lambda_{\rm int}{}^i$ are the mean path lengths for escape, decay, and interaction of nuclei of species i; $\lambda_{\rm spall}{}^{ki}$ and $\lambda_{\rm dec}{}^{ki}$ are the mean path lengths for spallation and decay of nuclei of species k into species i; $-w_i(E)$ is the mean energy loss per unit path length. Note that

$$\lambda_{\rm int,(spall)} = \frac{\langle m \rangle}{\sigma_{\rm int,(spall)}} , \qquad \text{and} \qquad \lambda_{\rm dec} = \gamma \tau_{\rm dec} \beta c n \langle m \rangle ,$$

where n and $\langle m \rangle$ are the mean number density and mass of interstellar nuclei encountered by the cosmic rays, taken to be 0.3 cm^{-3} and 1.3 amu, respectively.

In actual calculations, solutions $J_i{}^s(E, x)$ to the slab model equations,

$$\frac{\partial J_i{}^s(E, x)}{\partial x} + \frac{J_i{}^s(E, x)}{\lambda_{\rm dec}{}^i(E)} + \frac{J_i{}^s(E, x)}{\lambda_{\rm int}{}^i(E)} - \sum_{k \geq i} \left[\frac{J_k{}^s(E, x)}{\lambda_{\rm spall}{}^{ki}(E)} + \frac{J_k{}^s(E, x)}{\lambda_{\rm dec}{}^{ki}(E)} \right] + \frac{d}{dE}[w_i(E) J_i{}^s(E, x)] = 0 , \quad (2)$$

with initial conditions, $J_i{}^s(E, 0) = Q_i(E)$, may be obtained numerically:

$$J_i{}^s(E, x) = J_i{}^s(E_i, x - \Delta x) \frac{w_i(E_i)}{w_i(E)} \left[1 - \frac{\Delta x}{\lambda_{\rm int}{}^i(E)} - \frac{\Delta x}{\lambda_{\rm dec}{}^i(E)} \right] + \sum_{k \geq i} \frac{w_k(E_k)}{w_k(E)} J_k{}^s(E_k, x - \Delta x) \left[\frac{\Delta x}{\lambda_{\rm spall}{}^{ki}(E)} + \frac{\Delta x}{\lambda_{\rm dec}{}^{ki}(E)} \right] . \quad (3)$$

Here E_i is the energy of a nucleus of species i at path length $(x - \Delta x)$ such that its energy at path length x is E. E_i is obtained from range-energy tables, or, for small relative losses in energy, $E_i \approx E - w_i(E)\Delta x$.

The solutions $J_i(E)$ to the full equation may then be obtained from $J_i{}^s(E, x)$ by weighting with the path length distributions $P_i(x, E)$ (e.g., Lezniak 1979):

$$J_i(E) = \int_0^\infty J_i{}^s(E, x) P_i(x, E)\, dx . \quad (4)$$

For an exponential PLD, $P_i(x, E) = \exp[-x/\lambda_e{}^i(E)]$. For cross-checking purposes, when using an exponential path length distribution, we can include an additional term, $-\Delta x/\lambda_e{}^i(E)$, within the first bracket of equation (3) and use $P_i(x, E) = 1$ in equation (4).

For the spallation cross sections, we have used the Silberberg and Tsao semiempirical formulae and taken an interstellar medium consisting of 90% hydrogen and 10% helium by number. Some of the important cross sections at just a few of the energies used in our calculation for the spallation of ^{12}C and Fe are given in Tables 1 and 2. These cross sections include the effects of the decay of isotopes with half-lives less than 10^{13} s and should thus be considered the "cosmic ray cross sections." In each case the cross section given is in mb per average interstellar nucleus, and for Table 2 the cross sections have also been weighted with the expected abundances of Fe isotopes in the cosmic radiation. These tables illustrate the importance of using the observed energy dependence of the cross sections; e.g., the cross section for

TABLE 1

COSMIC RAY CROSS SECTIONS (mb) FOR THE SPALLATION OF ^{12}C INTO Li, Be, AND B

E(MeV/nucleon)	100	251	630	1584	3981
^{6}Li	15.8	15.8	15.3	14.4	14.4
^{7}Li	9.8	11.8	13.0	12.6	12.6
^{7}Be	11.5	12.0	11.7	10.5	10.5
^{9}Be	4.67	5.44	5.47	4.60	4.60
^{10}Be	1.28	2.17	3.06	3.04	3.04
^{10}B	37.5	32.6	27.2	22.4	22.4
^{11}B	82.1	61.5	70.0	62.9	61.4

TABLE 2

COSMIC RAY CROSS SECTIONS (mb) FOR THE SPALLATION OF Fe INTO SUB-Fe ELEMENTS

E(MeV/nucleon)	100	251	630	1584	3981
Sc	16.8	15.6	29.7	33.3	27.7
Ti	107.1	77.2	118.2	115.1	93.4
V	96.6	53.7	63.6	51.6	42.9
Cr	408.2	183.9	169.9	118.9	104.2
Mn[a]	271.7	144.0	114.0	94.2	92.8

[a] ^{54}Mn assumed stable.

production of Cr by spallation of Fe varies by a factor of 4 between 100 MeV/nucleon and high energies. Any error in the spallation cross sections will be directly reflected as an error in that predicted secondary-to-primary ratio.

Ionization losses are also very important in determining cosmic ray spectra at low energies and cannot be ignored. The effects of neglecting the energy dependence of the spallation cross sections and of neglecting ionization losses on the ratios of Fe secondaries to Fe and (Be + B) to C are illustrated in Figure 1 (for the model we adopt as our "standard" to be described later).

The total cross sections adopted also affect the predicted composition, particularly for heavy nuclei (e.g., sub-Fe/Fe ratio) where particle losses are dominated by nuclear interaction rather than escape. We use the energy independent fits to the data obtained by Hagen (1976):

$$\sigma_{\rm int} = 10\pi(1.29)^2\{A_T^{1/3} + A_B^{1/3} - 1.189 \exp\left[-0.05446 \min\left(A_T, A_B\right)\right]\}^2 \text{ mb}\,, \quad (5)$$

where A_T and A_B are the mass numbers of the target nuclei (interstellar matter) and the beam (cosmic ray nuclei). An energy-dependent total cross section scaled from the (p, p) cross section (Karol 1975) has been used by Garcia-Munoz *et al.* (1979) in their analysis. While perhaps theoretically justified, the present data are unable to determine the energy dependence with any certainty, and new measurements are urgently needed. The values used here (e.g., 716 mb for the p Fe total inelastic cross section) may be somewhat low. Values in the literature range from 721 ± 7 mb (Roberts *et al.* 1979) to 779 ± 27 mb (MacFall *et al.* 1979) for measurements at energies above 100 GeV, but the inelastic cross section rises with energy. The former cross section is an n Fe measurement and the latter a p Fe measurement. What is needed in our calculations is the mass-changing cross section (taking account of Fe → Fe + n), and the only measurement is 750 ± 50 mb (Westfall *et al.* 1979). Our adoption of the Karol (1975) energy-dependent form would reduce our predicted sub-Fe to Fe ratio by about ~ 10% above 400 MeV for the same grammage.

In our calculations we use the elemental source composition derived by Lezniak and Webber (1978) in conjunction with the isotopic abundances given by Cameron (1980). These are given in Table 3. Elemental abundances for Cl–K and

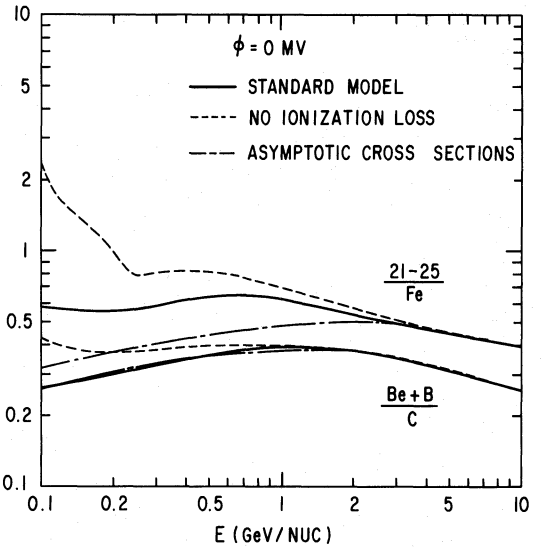

FIG. 1.—The interstellar ratios (Be + B)/C and (21 ≤ Z ≤ 25)/Fe predicted as a function of energy for the standard model (described later). The effect of neglecting ionization losses and the energy dependence of the spallation cross sections in propagation calculations is illustrated for particles outside the heliosphere ($\phi = 0$).

TABLE 3

PREDICTED COSMIC RAY COMPOSITION

ELEMENT	SOURCE	INTERSTELLAR ABUNDANCE AT GIVEN ENERGY (MeV/nucleon)				
		100	316	1000	3162	10000
Li	0	1.07	1.29	1.59	1.46	0.904
Be[a]	0	0.618	0.785	0.960	0.843	0.529
B	0	2.04	2.21	2.31	1.86	1.20
C	3.77	9.90	8.81	8.08	7.39	6.32
N	0.302	2.03	2.06	2.11	1.79	1.32
O	4.23	8.67	7.90	7.43	6.98	6.23
F	0.015	0.148	0.174	0.203	0.184	0.133
Ne	0.603	1.36	1.34	1.34	1.27	1.08
Na	0.026	0.170	0.191	0.213	0.201	0.151
Mg	0.892	1.61	1.56	1.55	1.49	1.33
Al	0.113	0.243	0.251	0.277	0.261	0.222
Si	0.872	1.28	1.25	1.28	1.24	1.15
P	0	0.021	0.031	0.054	0.051	0.035
S	0.140	0.230	0.254	0.319	0.307	0.257
Cl	0.001	0.024	0.037	0.066	0.059	0.041
Ar	0.028	0.089	0.115	0.176	0.158	0.118
K	0.001	0.044	0.065	0.114	0.097	0.069
Ca	0.060	0.153	0.183	0.249	0.213	0.171
Sc	0	0.031	0.039	0.057	0.045	0.033
Ti	0.006	0.132	0.151	0.189	0.144	0.111
V	0.001	0.070	0.073	0.079	0.058	0.046
Cr	0.031	0.212	0.199	0.188	0.147	0.127
Mn[b]	0.023	0.120	0.125	0.119	0.110	0.097
Fe[c]	1.0	1.0	1.0	1.0	1.0	1.0
Co	0	0.0008	0.0011	0.0014	0.0011	0.0010
Ni	0.042	0.037	0.037	0.038	0.038	0.039

[a] ^{10}Be assumed stable.
[b] ^{54}Mn assumed stable.
[c] Normalization.

Sc–Mn are also from Cameron (1980) but normalized to the upper limits given by Lezniak and Webber (1978) for these groups. All injection spectra are taken to be proportional to $W^{-2.3}$, where W is total energy per nucleon (Ormes and Freier 1978). The abundance ratios calculated depend on the injection spectra and primary composition adopted.

We have included the effects of solar modulation on the observed composition by using the "force field" solution (Gleeson and Axford 1968). The modulated spectra $J_i^m(E)$ are obtained from the interstellar spectra $J_i(E)$ at a given kinetic energy per nucleon E by

$$J_i^m(E) \approx \frac{E^2 + 2E}{(E + \Phi)^2 + 2(E + \Phi)} J_i(E + \Phi)\,, \tag{6}$$

where $\Phi = \phi(Ze/A)$ is the mean energy loss per nucleon in the heliosphere. We have usually used a deceleration parameter $\phi = 200$ MV as being typical of values derived from the data, although the effect of varying ϕ is discussed later.

We also consider the effect on composition of propagation through the atmosphere. For this we solve the slab model equations (eq. 3) with initial conditions $J_i^s(E, 0) = J_i^m(E)$. For the case of an experiment at a mean slant depth x_A in the atmosphere, we take a path length distribution $P(x) = \delta(x - x_A)$. In reality, this will be broadened by the finite acceptance solid angles of detectors, but, since this varies from experiment to experiment, we do not consider this effect here. The amount of atmospheric correction necessary can be seen in Figure 2. Here we present results of our calculations of the ratios (Be + B)/C and $(21 \leq Z \leq 25)$/Fe in interstellar space, above the atmosphere (effects of solar modulation with $\phi = 200$ MV) and at various depths in the atmosphere appropriate to balloon-borne experiments. These calculations are for our standard model (to be described in the next section). As can be seen, features in the ratios below $\sim$1 GeV/nucleon will be washed out in a few g cm^{-2} of atmosphere because of ionization losses.

III. INTERPRETATION OF Be, B, C COMPOSITION

The role of the ratio of (Be + B)/C is to determine the mean escape length as outlined in the introduction. Here we present the results of our calculations of the ratio (Be + B)/C as a function of energy for an exponential path length distribution. The results are shown in Figure 3 for various mean escape lengths. Here we have used a solar modulation deceleration parameter of $\phi = 200$ MV. We also show a survey of the data on this ratio corrected to the top of the

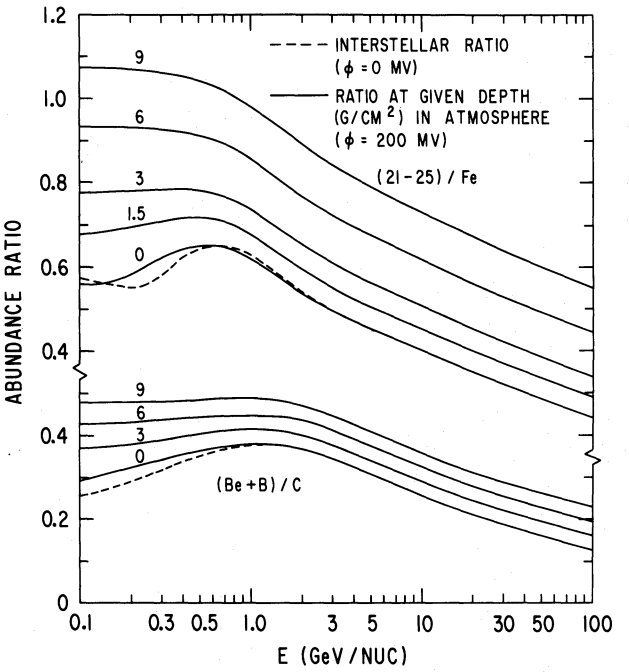

FIG. 2.—The ratios (Be + B)/C and $(21 \leq Z \leq 25)$/Fe predicted for the standard model outside the heliosphere, above the atmosphere (effect of solar modulation) and at the depths indicated (g cm^{-2}) in the atmosphere.

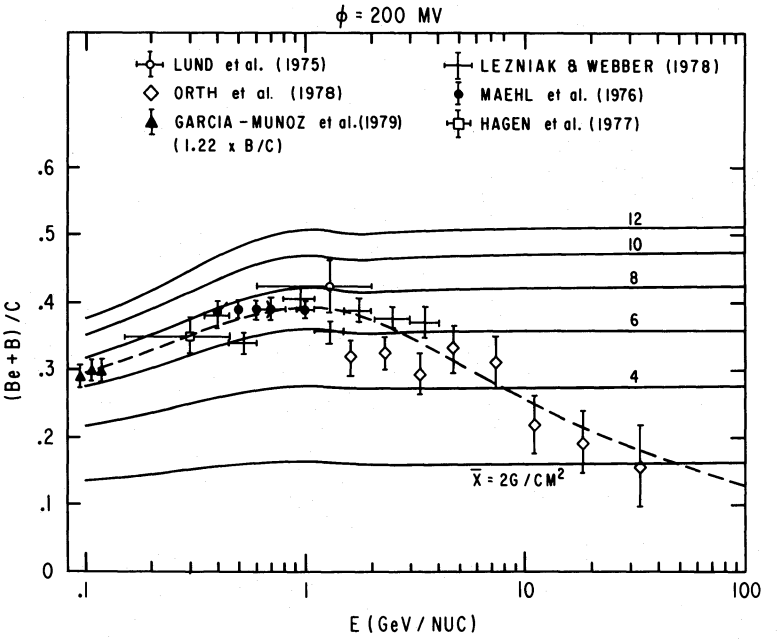

FIG. 3.—The (Be + B)/C ratio predicted for an exponential path length distribution for the mean escape lengths (g cm^{-2}) indicated. The effects of solar modulation with $\phi = 200$ MV are included. The experimental data have been corrected for propagation through the atmosphere.

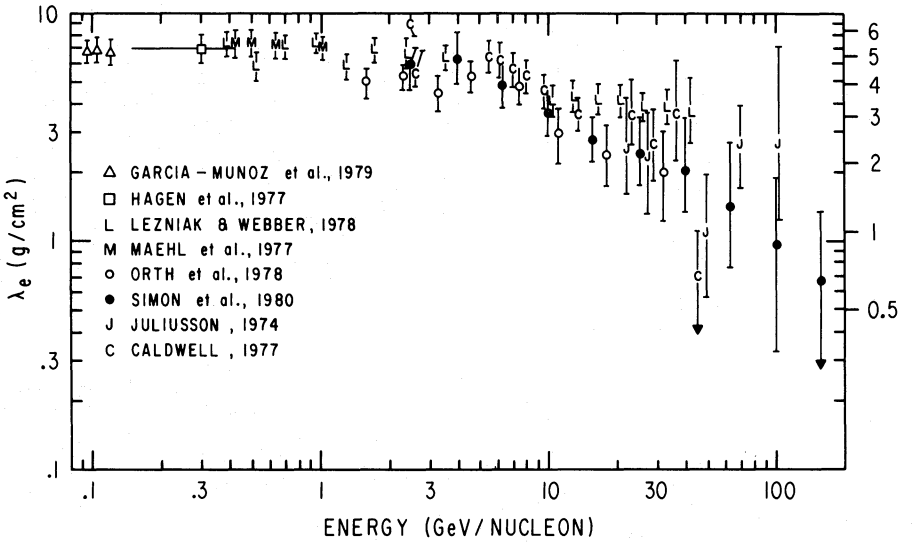

FIG. 4.—The variation of mean escape length with energy based on our interpretation of the (Be + B)/C ratio and the B/C ratio. The scale at the right of the figure gives the mean escape length for the most extreme two-zone model (discussed later in the text).

atmosphere (in most cases by the original authors). These predictions have been used to derive a mean escape length for each datum point, and Figure 4 shows the variation of mean escape length with energy obtained in this way. Above 2 GeV/nucleon the data are generally interpreted as suggesting that the mean escape length is proportional to $E^{-0.4\pm0.1}$. Below 2 GeV/nucleon we find that the mean path length is essentially independent of energy at ~ 7 g cm^{-2}. This conclusion is based on the data at the lowest energies considered ($\sim$ 100 MeV/nucleon) and is thus sensitive to the amount of solar modulation adopted ($\phi = 200$ MV) and to the shape of the injection spectrum. The data at $\sim$1 GeV/nucleon, where solar modulation is not too important, fix the escape length at about ~ 7 g cm^{-2}, but at energies $\sim$ 100 MeV/nucleon an escape length as high as 9 g cm^{-2} (no solar modulation) or as low as 5 g cm^{-2} ($\phi = 400$ MV) is also possible. For our "standard model" we therefore adopt

$$\lambda_e(E) = \begin{cases} 7 \text{ g cm}^{-2}, & E < 2 \text{ GeV/nucleon}; \\ 7(E/2 \text{ GeV nucleon})^{-0.4} \text{ g cm}^{-2}, & E \geq 2 \text{ GeV/nucleon}; \end{cases} \quad (7)$$

for all species with $Z > 2$. Predictions of the ratio (Be + B)/C based on this standard model are shown by the dashed curve of Figure 3.

The energy dependence of the mean escape length above is not expected to be valid at the highest energies. For example, the mechanisms responsible for this energy dependence would almost certainly break down at energies for which equation (7) would give a mean escape length less than the thickness of the galactic disk. Some information about the high energy behavior may be obtained from measurements of the anisotropy of cosmic rays. Provided the streaming of cosmic rays is not much in excess of that necessary to transport the cosmic ray nuclei from the sources to the escape boundary, then the magnitude of the expected anisotropy is given by (Kiraly *et al.* 1979*a*):

$$\xi = t_{DE}/t_{con}, \quad (8)$$

where t_{con} is the confinement time of cosmic rays in the Galaxy and t_{DE} is the "direct exit" time, i.e., the escape time of neutral cosmic rays. Since the confinement time is proportional to escape length, the anisotropy would be inversely proportional to escape length. The measured anisotropy is almost constant at $\sim 0.05\%$ over the energy range 5×10^2 GeV/nucleus to 5×10^4 GeV/nucleus (see the review by Elliot 1979), and this has been used by Kiraly *et al.* (1979*b*) to infer that the mean escape length is essentially constant over this energy range. On the other hand, the absence of any flattening in the cosmic ray proton spectrum up to 2 TeV/nucleon suggests that the energy-dependent escape mechanisms continues to at least that energy. Any flattening in the particle spectrum which might be observable in the 100 TeV range could be associated with a change in the escape mechanism.

The abundances of the elements Li through Ni predicted at various energies for the standard model are given alongside the source abundances in Table 3. Using this model we can look at other abundance ratios to see whether they are consistent with the experimental results. In Figure 5 we reproduce the survey of data on the ratio $(17 \leq Z \leq 25)/(26 \leq Z \leq 28)$ from Simon *et al.* (1980). This is compared with the ratio predicted for the standard model in the figure. The energy dependence of the predicted ratio is in good agreement with the observations, bearing in mind the statistical uncertainties. In particular, we are able to reproduce the observed peak in the abundance ratio at $\sim$ 1 GeV/nucleon.

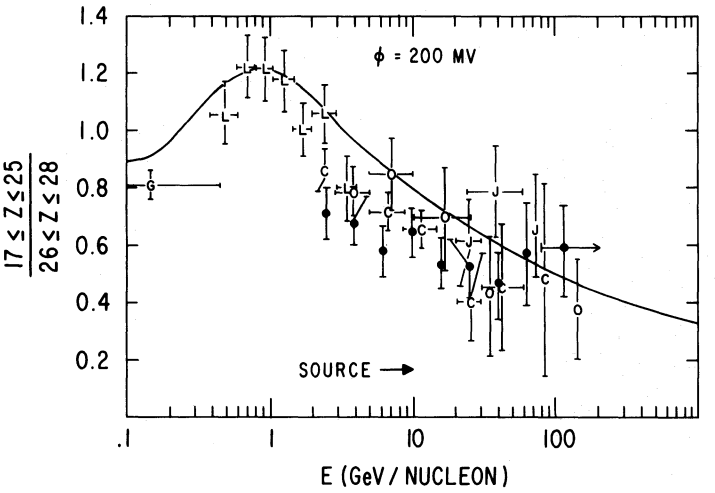

FIG. 5.—A survey of data on the ratio $(17 \le Z \le 25)/(26 \le Z \le 28)$ is compared with our prediction for the standard model (solar modulation with $\phi = 200$ MV is included). The symbols are as follows: G, Garcia-Munoz *et al.* (1977); L. Lezniak and Webber (1978); J, Juliusson (1974); O, Orth *et al.* (1978); filled circle, Simon *et al.* (1980).

From the variation of the ratio of two "primary" components with energy we can look for variations in the slope of injection spectra between the different elements. A survey of measurements of the Fe/O ratio is given in Figure 6, and it is seen that, despite the large amount of scatter between the data, this ratio increases from ~ 0.8 at 100 MeV/nucleon to ~ 1.5 at 100 GeV/nucleon. The predicted ratio also increases with energy due to the energy dependence of the relative importance of escape and interaction losses, especially for Fe nuclei. At very high energies, since losses are dominated by escape ($\lambda_e \ll \lambda_{\rm int}$) for both species, the Fe/O ratio approaches the source ratio. Below ~ 1 GeV/nucleon, the ratio is also reduced by ionization losses. These effects are further enhanced for observations made from balloons in the atmosphere. The predicted ratio is shown in Figure 6 for depths of 3, 6, and 9 g cm^{-2} in the atmosphere. The scatter in the data is quite large and could arise partly from the use of different atmospheric correction factors by the various authors. Within the uncertainties in the data we do not detect any significant difference between the injection spectra of Fe and O; in this energy range the observed flattening can be explained solely by propagation effects as noted by Cowsik and Wilson (1973). A lower Fe/O source ratio may, however, be indicated by the low energy satellite measurement.

IV. "TWO-ZONE" OR "NESTED LEAKY BOX" MODELS

The composition of heavy nuclei is particularly sensitive to the *shape* of the path length distribution because the interaction mean free paths of heavy nuclei are much less than the mean escape length (e.g., $\lambda_{\rm int}^{\rm Fe} \approx 2.6$ g cm^{-2}). Thus, if the path length distribution were truncated for small path lengths, then nuclear interactions would have a greater effect in

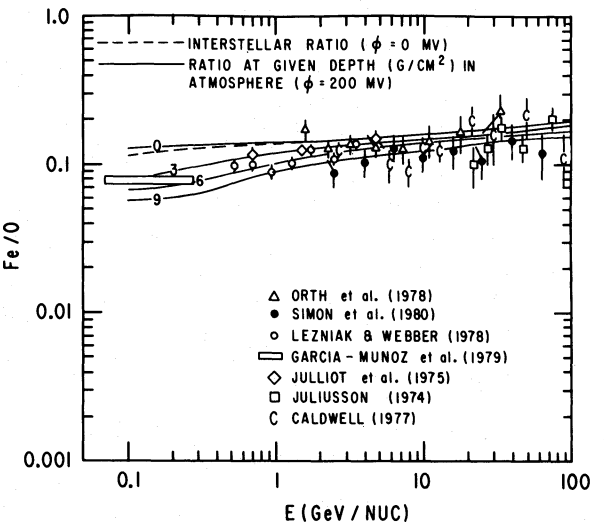

FIG. 6.—A survey of data on the Fe/O ratio is compared with our prediction for the standard model. The effect of solar modulation and propagation through 3, 6, and 9 g cm^{-2} of atmosphere is indicated.

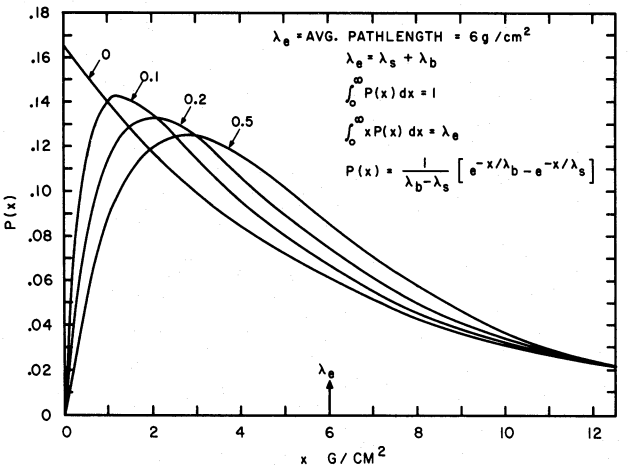

FIG. 7.—The shape of the path length distribution in the two-zone model for various values of λ_s/λ_e, keeping λ_e fixed

determining the observed composition, resulting in a significantly higher ratio of secondary nuclei to primary nuclei. A similar effect, although not so pronounced, results for the composition of light and medium nuclei, increasing, e.g., the (Be + B)/C ratio observed, and this must be taken into account when deriving the mean escape length from the data for such models.

Cowsik and Wilson (1973, 1975) have shown that "two-zone" or "nested leaky box" models result in a PLD which is the convolution of two exponential distributions. We use the formalism introduced by Simon (1977) to give physical meaning to a parameter which describes the shape of the PLD. The distribution is uniquely defined by two parameters: the mean path length in the source region λ_s, and the mean path length in the galaxy λ_b (the mean escape length is $\lambda_e = \lambda_s + \lambda_b$, and the ratio λ_s/λ_e determines the shape of the distribution). Path length distributions for λ_s/λ_e ranging from 0.0 (pure exponential PLD) to 0.5 (for λ_s/λ_e values greater than 0.5, the shape of the distribution is the same as for $1.0 - \lambda_s/\lambda_e$) are shown in Figure 7 for $\lambda_e = 6\ \mathrm{g\ cm^{-2}}$. We use the ratio λ_s/λ_e here as a convenient parametrization of the shape of the PLD. Once the shape has been determined experimentally, it can be compared with different cosmic ray storage models (Lezniak and Webber 1979) or source distributions (Owens 1976).

The variation of the B/C and (Be + B)/C ratios with mean escape length λ_e is given in Figure 8 for various values of

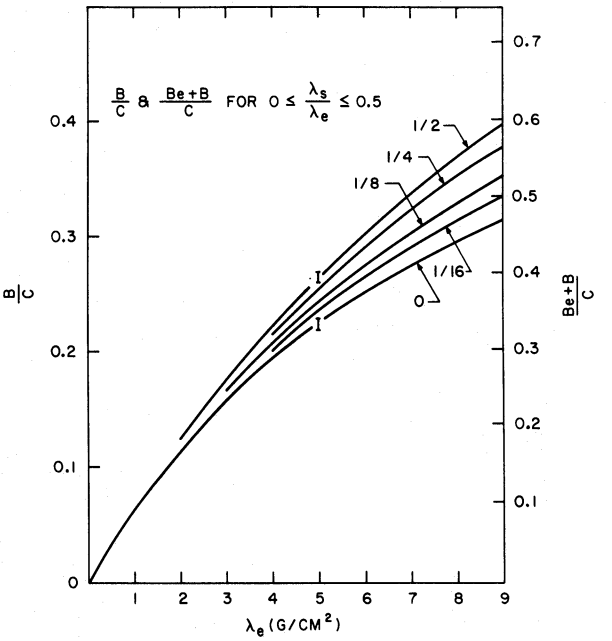

FIG. 8.—The variation of B/C and (Be + B)/C at high energies with λ_e for the two-zone model for various values of λ_s/λ_e (*the numbers attached to the curves*).

λ_s/λ_e. The calculations for this figure were done using the asymptotic cross sections and correspond to energies above 4 GeV nucleon. The cross sections are, however, almost independent of energy above 1 GeV. This is fortunate since the (Be + B)/C ratio is best known at around 1–2 GeV/nucleon, and we shall use this to fix λ_e for different values of λ_s/λ_e. From Figure 8 we see that λ_e could vary from 5.2 g cm^{-2} ($\lambda_s/\lambda_e = 0.5$) to 7.0 g cm^{-2} ($\lambda_s/\lambda_e = 0$), depending on the shape of the PLD, and give the observed (Be + B)/C ratio between 1 and 2 GeV/nucleon.

We have calculated the ratio of iron secondaries ($21 \leq Z \leq 25$) to Fe and (Be + B)/C as a function of energy for two different cases: the standard model ($\lambda_s/\lambda_e = 0$; $\lambda_e = 7$ g cm^{-2} below 2 GeV/nucleon, $7(E/2)^{-0.4}$ g cm^{-2} above 2 GeV/nucleon) and for a severly truncated PLD ($\lambda_s/\lambda_e = 0.33$; $\lambda_e = 5.3$ g cm^{-2} below 2 GeV/nucleon, $5.3(E/2)^{-0.4}$ g cm^{-2} above 2 GeV/nucleon). The predictions are shown in Figure 9. In the figure, we also show the effect of varying the amount of solar modulation and give results for $\phi = 0$, 200 MV, and 400 MV. The predictions for the ($21 \leq Z \leq 25$)/Fe ratio may be compared with a survey of the experimental results shown in the figure. From this comparison, it appears that there is no need to invoke a truncated path length distribution to explain the observed ratio. The data are consistent with the predictions for the exponential PLD; however, because of the large amount of scatter between data points, we cannot rule out the possibility of small values of λ_s/λ_e. As can be seen from Figure 9, an increase of 10% in the cross sections would reduce these curves by 10% but would not alter this conclusion.

A different conclusion has been reached by the Chicago group (Garcia-Munoz *et al.* 1979). These authors require a PLD of the form exp $(-x/X_0)$ with $X_0 = 5$ g cm^{-2} of hydrogen (6 g cm^{-2} of interstellar material) and truncated with a linear rise between 0 and 1.3 g cm^{-2} (hydrogen) to fit both the B/C and sub-Fe/Fe ratios from 500 MeV/nucleon to 1 GeV/nucleon. At lower energies they require a lower value of X_0. The discrepancy between this result and our analysis is due mainly to differences in the total (as noted earlier) and spallation cross sections adopted. This underlines the necessity for new cross section measurements. Another difference is in the shape of the injection spectra used. Garcia-Munoz *et al.* (1979) have adopted $(E + 400$ MeV/nucleon$)^{-2.6}$ as opposed to our $(E + 938$ MeV/nucleon$)^{-2.3}$. This difference is only important at low energies (< 500 MeV/nucleon) where ionization losses and solar modulation are important. Their spectra will clearly be too steep at high energies once energy-dependent leakage is taken into account.

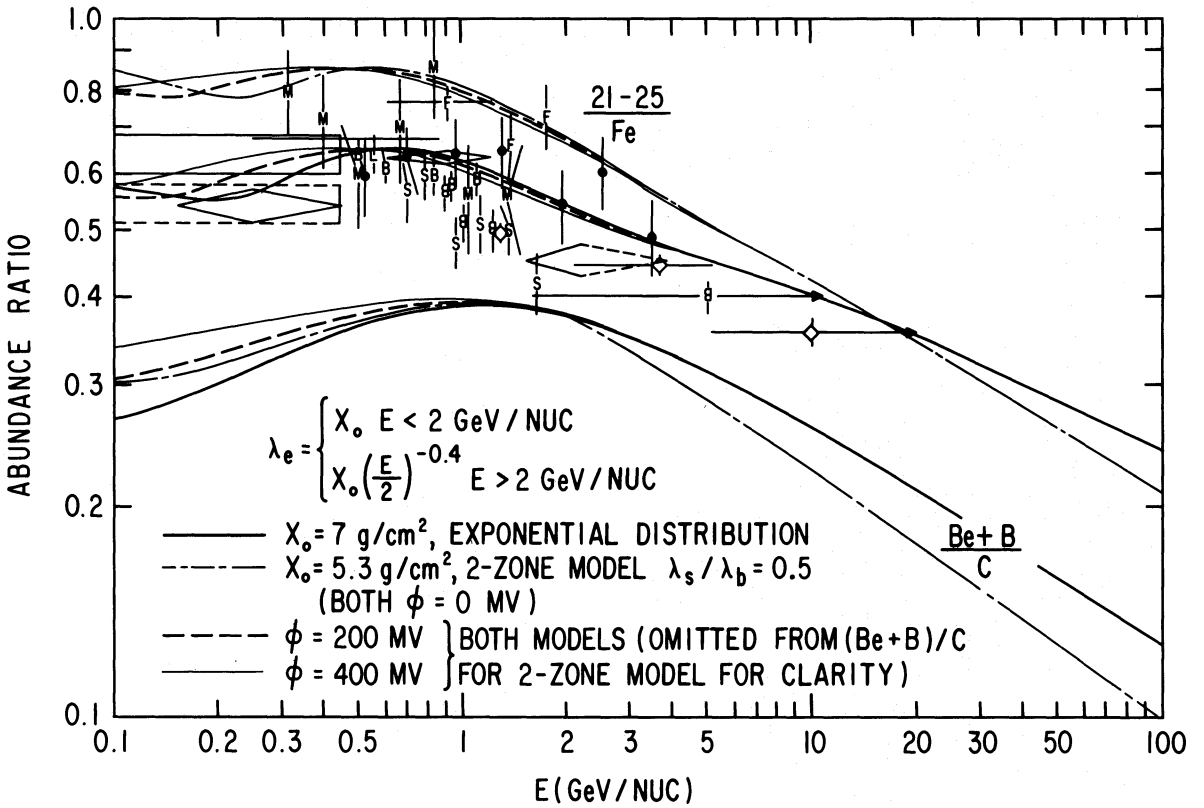

FIG. 9.—The variation with energy of the ratios (Be + B)/C and ($21 \leq Z \leq 25$)/Fe for the standard model and for the two-zone model with $\lambda_s/\lambda_e = 0.33$. Separate curves are given for $\phi = 0$, 200 MV, and 400 MV. Symbols for the experimental data on the ($21 \leq Z \leq 25$)/Fe ratio are as follows: M, Maehl *et al.* (1977); L, Lund *et al.* F, Freier *et al.* (1979); B and B, Benegas *et al.* (1975); S, Scarlett, Freier, and Waddington (1978); small diamond, Copenhagen-Saclay collaboration (1980) (preliminary *HEAO 3* data); filled circle, Lezniak and Webber (1978); large diamond, Israel *et al.* (1979); rectangle, Garcia-Munoz *et al.* (1979); dashed rectangle, Garcia-Munoz *et al.* (1977).

V. ABUNDANCE OF INDIVIDUAL IRON SECONDARIES

Using our standard model, we have calculated the expected abundances of the elements Sc, Ti, V, Cr, and Mn relative to Fe as a function of energy. The results are shown in Figures 10*a–c*, where they are compared with the available data. As can be seen, the predicted abundance ratios are in overall reasonable agreement with the data. In particular, the energy dependence of abundance ratios from the preliminary data from the *HEAO 3* experiment (Copenhagen-Saclay collaboration 1980) is adequately reproduced with the exception of the Mn/Fe ratio which is less steep than that predicted for ^{54}Mn stable against β-decay. That may be due to the survival of ^{54}Mn above a few tens of GeV/nucleon and almost complete decay below ~ 1 GeV/nucleon as shown in Figure 10*a*. We also show our prediction for a mean lifetime of ^{54}Mn against β-decay of 2×10^6 yr (Cassé 1973) and propagation in a medium of mean density 0.33 atoms cm^{-3} (Wiedenbeck and Greiner 1980). This gives an acceptable fit to the *HEAO 3* data although a better fit would result for a shorter decay time or a less dense propagation region.

Because of the large uncertainties attached to the measurements of the spallation cross sections, it is difficult to go further at the present time. Clearly there is interesting structure in these cross sections which should be observable in the abundance ratios of Fe secondaries. Indeed, if a pronounced maximum occurred in a particular cross section at several

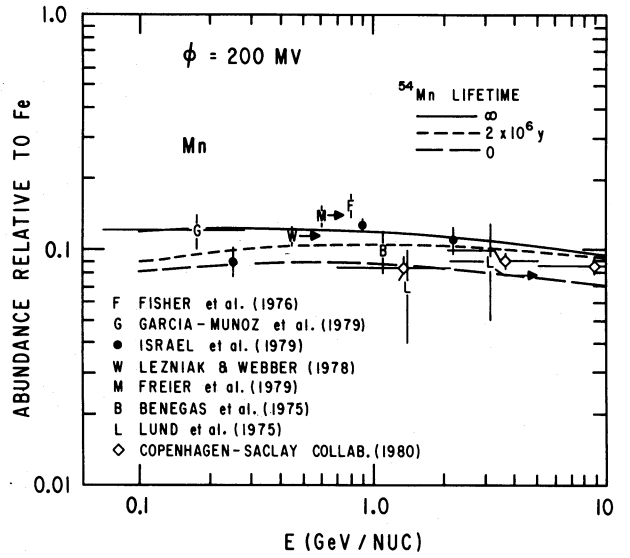

FIG. 10*a*

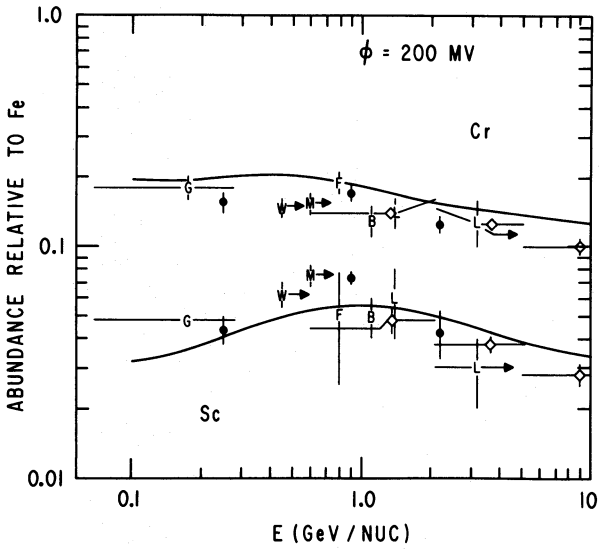

FIG. 10*b*

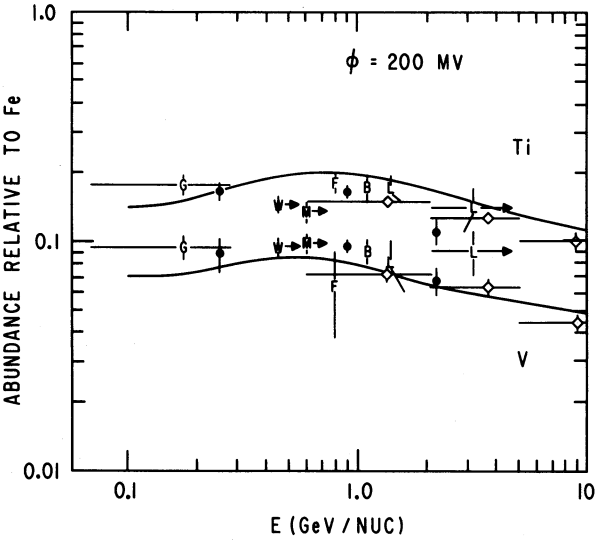

FIG. 10*c*

FIG. 10.—The predicted and observed abundance of individual Fe-secondary elements: (*a*) Mn; (*b*) Cr and Sc; (*c*) Ti and V

hundred MeV/nucleon, it may be possible to obtain a "direct measurement" of the amount of solar modulation by determining the energy at which the abundance of that species relative to Fe was greatest. The displacement in energy of this peak relative to that in the spallation cross sections would, after correcting for the effect of ionization losses in the interstellar medium, etc., be equal to the mean energy lost in the heliosphere, Φ. Detailed measurements of the relative abundances of individual Fe-secondary isotopes may be more suitable for this study. This is because features in cross sections of individual isotopes are expected to be more pronounced than in cross sections for the production of a group of isotopes which contain the superposition of features at different energies. Cosmic ray data with sufficiently good statistics to measure ratios of individual nuclei to iron as a function of energy to 3% accuracy should soon be available from the *HEAO 3* satellite experiments. This data should be able to determine λ_s to an accuracy of ~ 0.3 g cm^{-2}. Before such studies can be completed, it will be necessary for new and more accurate measurements of the energy dependence of the spallation cross sections to be made.

VI. INJECTION SPECTRA

As noted earlier, the previous interpretation of the observed energy spectra (Ormes and Freier 1978) in terms of injection spectra of the form $W^{-2.3}$, where W is the total energy per nucleon, needs some revision in order to take into account ionization losses in the interstellar medium and solar modulation. In Figure 11, we give a survey of recent observations of the energy spectrum of C and Fe. Predictions for the standard model ($W^{-2.3}$ spectrum) with $\phi = 0$, 200 MV, and 400 MV and for injection spectra proportional to $R^{-2.3}$ (where R is rigidity) with $\phi = 200$ MV are also shown. For the degree of solar modulation usually assumed (i.e., $\phi = 200$ MV), the predicted spectra are seen to be too flat at low energies for the $W^{-2.3}$ model and too steep for the $R^{-2.3}$ model. It seems that the injection spectra must lie between these two forms.

VII. SUMMARY

We have calculated the composition of cosmic rays above 100 MeV/nucleon expected for different path length distributions and compared our predictions with the data available. Our calculations include the effects of the energy dependence of the spallation cross sections, ionization losses, solar modulation, and propagation through the atmosphere down to balloon altitudes.

We find that an exponential path length distribution is able to account for the ratios of secondary-to-primary nuclei observed in the cosmic radiation from 100 MeV/nucleon to several hundred GeV/nucleon, provided the escape length is ~ 7 g cm^{-2} below 2 GeV/nucleon and proportional to $E^{-0.4\pm0.1}$ at higher energies. Below 500 MeV/nucleon the cosmic ray composition is most sensitive to the shape of the injection spectrum and solar modulation. The shape of the PLD is best measured between 500 MeV/nucleon and 2 GeV/nucleon and, with the advent of the *HEAO 3* results, will be limited

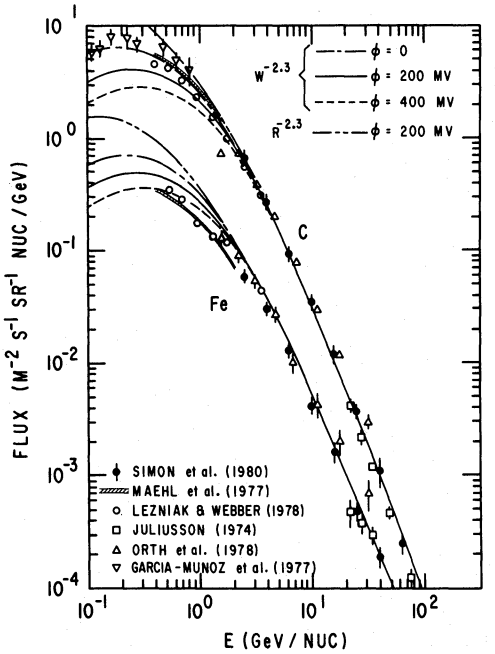

FIG. 11.—The measured fluxes of Fe and C are compared with the predictions for the standard model with $\phi = 0$, 200 MV, and 400 MV. Also given are predictions for an injection spectrum which is a power law in rigidity. The curves are normalized such that the flux of C at 10 GeV/nucleon is 3.2×10^{-2} m^{-2} s^{-1} sr^{-1} (GeV/nucleon)$^{-1}$.

by our knowledge of both the partial and total cross sections, particularly for interactions of iron nuclei. At energies above ~ 2 GeV/nucleon the energy dependence of the escape length dominates. Using our standard model we predict abundances of the individual Fe secondaries which are consistent with the data available and generally lie $\sim 10\%$ above the preliminary *HEAO 3* data. A 10% increase in the total cross sections would improve the agreement for most of the individual elements, and the general trend of the predicted energy dependence seems to be tracked by the data. An extreme of half the cosmic ray matter being around the source $\lambda_s = 2.6$ g cm^{-2} seems to be ruled out by these data; however, any value of $\lambda_s \lesssim 1$ g cm^{-2} is possible within the limits of the data, the cross sections, and these calculations.

When better data on Fe-secondary abundances from *HEAO 3* become available, more refined tests will be possible; however, it will be necessary first to determine the energy dependence of the (Be + B)/C ratio and hence the energy dependence of the escape length with greater precision. In addition, new measurements of the energy dependence of both the total and the spallation cross sections of Fe are vital if the subiron cosmic ray data are to be used to more accurately determine the shape of the path length distribution.

We acknowledge Drs. R. Silberberg and C. H. Tsao for their help with cross sections. We also thank Dr. P. Freier for her enthusiasm, encouragement, and interest in this work and for her efforts to sort out cosmic ray propagation problems.

REFERENCES

Benegas, J. C., Israel, M. H., Klarmann, J., and Maehl, R. C. 1975, *Proc. 14th Internat. Cosmic Ray Conf.*, Vol. **1**, p. 251.
Blandford, R. C., and Ostriker, J. P. 1978, *Ap. J. (Letters)*, **221**, L29.
Caldwell, J. H. 1977, *Ap. J.*, **218**, 269.
Cameron, A. G. W. 1980, Center for Astrophysics preprint, No. 1357.
Cassé, M. 1973, *Ap. J.*, **180**, 623.
Copenhagen-Saclay collaboration. 1980, Preliminary Results on the Elemental Abundances of Cosmic Ray Nuclei in the Iron Peak, presented at APS and COSPAR meetings.
Cowsik, R., and Wilson, L. W. 1973, *Proc. 13th Internat. Cosmic Ray Conf.*, Vol. **1**, p. 500.
———. 1975, *Proc. 14th Internat. Cosmic Ray Conf.*, Vol. **2**, p. 659.
Cowsik, R., Yash Pal, Tandon, S. N., and Verma, R. P. 1967, *Phys. Rev.*, **158**, 1238.
Eichler, D. 1980, *Ap. J.*, **237**, 809.
Elliot, H. 1979, *Proc. 16th Internat. Cosmic Ray Conf.*, Vol. **14**, p. 200.
Fichtel, C. E., and Reames, D. E. 1968, *Phys. Rev.*, **175**, 1564.
Fisher, A. J., Hagen, F. A., Maehl, R. C., Ormes, J. F., and Arens, J. F. 1976, *Ap. J.*, **205**, 938.
Freier, P. S., Young, J., Waddington, C. J., Fickle, R., Gilman, C., and Scarlett, W. R. 1979, *Proc. 16th Internat. Cosmic Ray Conf.*, Vol. **1**, 316.
Garcia-Munoz, M., Margolis, S. H., Simpson, J. A., and Wefel, J. P. 1979, *Proc. 16th Internat. Cosmic Ray Conf.*, Vol. **1**, p. 310; **13**, 401.
Garcia-Munoz, M., Mason, G. M., and Simpson, J. A. 1977, *Proc. 15th Internat. Cosmic Ray Conf.*, Vol. **1**, 224.
Garcia-Munoz, M., Mason, G. M., Simpson, J. A., and Wefel, J. P. 1977, *Proc. 15th Internat. Cosmic Ray Conf.*, Vol. **1**, p. 230.
Garcia-Munoz, M., and Simpson, J. A. 1970, *Acta Physica Hungaricae*, **29**, 318.
Gleeson, L. J., and Axford, W. I. 1968, *Ap. J.*, **154**, 1011.
Hagen, F. A. 1976, Ph.D. thesis, University of Maryland.
Hagen, F. A., Fisher, A. J., and Ormes, J. F. 1977, *Ap. J.*, **212**, 262.
Israel, M. H., Klarmann, J., Love, P. L., and Tueller, J. 1979, *Proc. 16th Internat. Cosmic Ray Conf.*, Vol. **1**, p. 323; **13**, p. 402.
Jokipii, J. R. 1976, *Ap. J.*, **208**, 900.
Jokipii, J. R., and Higdon, J. C. 1979, *Ap. J.*, **228**, 293.
Jones, F. C. 1979, *Ap. J.*, **229**, 747.
Juliusson, E. 1974, *Ap. J.*, **191**, 331.
Julliot, C., Koch, L., and Petrou, N. 1975, *Proc. 14th Internat. Cosmic Ray Conf.*, Vol. **12**, p. 4118.
Karol, P. J. 1975, *Phys. Rev., C*, **11**, 1203.
Kiraly, P., Kota, J., Osborne, J. L., Stapley, N. R., and Wolfendale, A. W. 1979*a*, *Revista del Nuovo Cimento*, **2** (Serie 3), No. 7.
———. 1979*b*, *Proc. 16th Internat. Cosmic Ray Conf.*, Vol. **4**, p. 221.
Lezniak, J. A. 1979, *Ap. Space Sci.*, **63**, 279.
Lezniak, J. A., and Webber, W. R. 1978, *Ap. J.*, **223**, 676.
———. 1979, *Ap. Space Sci.*, **63**, 35.
Lund, N., Rasmussen, I. L., Peters, B., Rotenberg, M., and Westergaard, N. J. 1975, *Proc. 14th Internat. Cosmic Ray Conf.*, Vol. **1**, p. 263.
MacFall, J. R., Ellsworth, R. W., Ito, A. S., Siohan, F., Streitmatter, R. E., Tonwar, S. C., Viswanath, P. R., and Yodh, G. B. 1979: *Nucl. Phys., B*, **151**, 213.
Maehl, R. C., Ormes, J. F., Fisher, A. J., and Hagen, F. A. 1977: *Ap. Space Sci.*, **47**, 163.
Ormes, J. F., and Freier, P. S. 1978, *Ap. J.*, **222**, 471.
Orth, C. D., Buffington, A., Smoot, G. F., and Mast, T. S. 1978, *Ap. J.*, **226**, 1147.
Owens, A. J. 1976, *Ap. Space Sci.*, **40**, 357.
Raisbeck, G. M. 1979, *Proc. 16th Internat. Cosmic Ray Conf.*, Vol. **14**, 146.
Roberts, T. J., Gustafson, H. R., Jones, L. W., Longo, J. F., and Whalley, M. R. 1979, *Nucl. Phys., B*, **159**, 56.
Scarlett, W. R., Freier, P. S., and Waddington, C. J. 1978, *Ap. Space Sci.*, **59**, 301.
Scott, J. S., and Chevalier, R. A. 1975, *Ap. J. (Letters)*, **197**, L5.
Shapiro, M. M., and Silberberg, R. 1970, *Ann. Rev. Nucl. Sci.*, **20**, 323.
Shapiro, M. M., Silberberg, R., and Tsao, C. H. 1973, *Proc. 13th Internat. Cosmic Ray Conf.*, Vol. **1**, p. 578.
Silberberg, R., and Tsao, C. H. 1973*a*, *Ap. J. Suppl.*, **25**, 315.
———. 1973*b*, *Ap. J. Suppl.*, **25**, 335.
———. 1977*a*, *Ap. J. Suppl.*, **35**, 129.
———. 1977*b*, *Ap. J. Suppl.*, **35**, 137.
———. 1977*c*, *Proc. 15th Internat. Cosmic Ray Conf.*, Vol. **2**, p. 84.
Simon, M. 1977, *Astr. Ap.*, **61**, 833.
Simon, M., Spiegelhauer, H., Schmidt, W. K. H., Siohan, F., Ormes, J. F., Balasubrahmanyan, V. K., and Arens, J. F. 1980, *Ap. J.*, **239**, 712.
Tsao, C. H., and Silberberg, R. 1979, *Proc. 16th Internat. Cosmic Ray Conf.*, Vol. **2**, p. 202.
Westfall, G. D., Wilson, L. W., Lindstrom, P. J., Crawford, H. J., Greiner, D. E., and Heckman, H. H. 1979, *Phys. Rev., C*, **19**, 1309.
Wiedenbeck, M E., and Greiner, D. E. 1980, *Ap. J. (Letters)*, **239**, L139.

R. J. Protheroe and J. F. Ormes: Code 661, NASA Goddard Space Flight Center, Greenbelt, MD 20771

G. M. Comstock: Cosmo Science Associates, 21 Erland Road, Stony Brook, NY 11790